

Simulation of nozzle plume droplet flow in transitional regime

Yu.P.Golovachov^{*}, M.S.Ivanov⁺, D.V.Khotyanovskii⁺, A.N.Kudryavtsev⁺,
E.Yu.Kumzerova^{*}, A.A.Schmidt^{*}

^{}- Ioffe Physical Technical Institute of Russian Academy of Sciences,
Saint Petersburg, 194021, Russia*

*⁺- Institute of Theoretical and Applied Mechanics,
Siberian Division of Russian Academy of Sciences,
Novosibirsk 630090, Russia*

Abstract. The paper is focused on development and validation of an Euler-Lagrange algorithm for numerical simulation of droplet nozzle and plume flows. The Euler-Lagrange description of the medium implies utilization of appropriate models for the carrier phase and the probe particle model for the dispersed phase. A procedure of the two-way coupling between the phases implementing a special temporal-spatial averaging is described. Droplet evaporation is taken into account. Special attention is paid to model validation. Effect of droplet size is considered.

Keywords: Droplet flow, evaporation, supersonic flow, nozzle, jet, rarefied flow.

PACS: 47.55.Ca, 47.55.D-, 47.61.Jd

INTRODUCTION

Information on processes occurring in multiphase nozzle and plume flows is important in many fields of space technology. In particular, data on droplet flow structure are necessary for development of protection of a spacecraft from droplets produced by control thrusters. This study is a continuation of the previously conducted investigations of droplet nozzle and plume flows [1, 2]. Numerical simulation of such flows should be based on an adequate mathematical model accounting for interphase mass, momentum, and energy transfer.

One of the most efficient and flexible approach to simulation of two-phase flows is an Euler-Lagrange description utilizing separate consideration of the phases on the basis of appropriate models for the carrier phase and the probe particle model for the dispersed phase. To calculate spatial distributions of gas-dynamic functions of the dispersed phase and phase coupling terms a procedure of temporal-spatial averaging of trajectory parameters of the probe particles in each computational cell was implemented.

In this study at the Euler stage of the algorithm the carrier phase was assumed to be a compressible viscous gas with a constant specific heat ratio, most calculations of the gas flows were carried out using the Navier-Stokes equations. Transitional flow regimes were considered. Rarefaction effects were taken into account imposing velocity slip and temperature jump boundary conditions on solid flow boundaries. The equations were solved with a shock-capturing MUSCL TVD scheme. The HLLC approximate Riemann solver was used to calculate the inviscid fluxes, while the second-order central finite differences were utilized for the viscous terms. Time stepping was performed with the explicit Runge-Kutta scheme. In the most details this algorithm is described in [1].

The probe particle model of the Lagrange stage of the algorithm provides description of motion, heating, and evaporation/condensation of droplets. Phenomenological approach is used to close the model; the closing relations are based on experimental data on mass, momentum, and energy interphase transfer. Depending on probe droplet size the set of ordinary differential equations of Lagrange stage can be stiff one. To deal with such equations, the Adams method of integration is implemented.

Detailed description of algorithm of the Lagrange stage, discussion closing relations for the interphase drag, heat and mass transfer, as well as discussion of possible regimes of the droplet flows accounting for droplet deformation and break-up is presented in [2]. Analysis of the droplet drag, heat and mass transfer, droplet stability was based on

phenomenological considerations of the processes [3 – 12]. Special attention was paid to regimes characterized by moderate and high Knudsen numbers (see, for example, [4, 5, 11, 12]).

SOME RESULTS

Model Validation

To validate the proposed algorithm a set of simulations were carried out: 1) heating and evaporation of quiescent droplets and droplet in a convective flow of in ambient air [13]; 2) angular distribution of droplet mass flux in a nozzle plume [14]. Comparison of the obtained results with experimental data demonstrated good agreement.

Figure 1 presents results of computations obtained in the framework of the proposed algorithm. Motion of kerosene droplet in air was simulated, the air temperature was $T_g = 1000$ K, the ambient pressure was $p_g = 10^5$ Pa, initial droplet temperature and diameter were $T_d = 300$ K and $D_d = 1$ mkm, correspondingly, droplet velocity was $V_d = 10 - 100$ m/s. Comparison of the predictions with the experimental data [13] demonstrates rather good agreement for the droplet temperature, (b), (odds does not exceed 5%), while for submicron droplets ($D_p < 0.5$ mkm) the model underestimates the evaporation rate, (a).

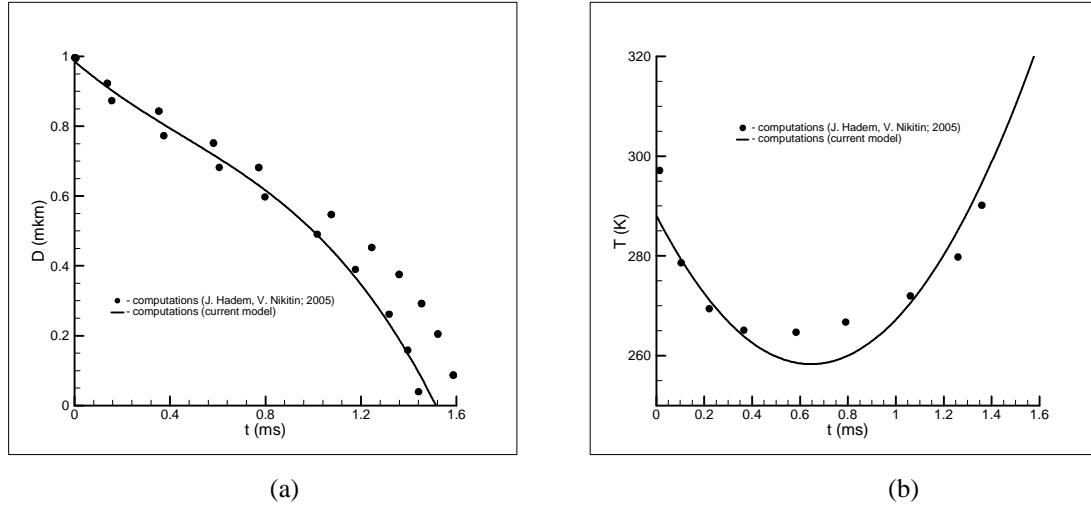


FIGURE 1. Variation in time of the droplet diameter, (a), and the droplet temperature, (b).

The angular distribution of the droplet mass flux in a plume flow corresponds to conditions [14] was simulated using the proposed algorithm. The main contribution to the mass flux is provided by droplets of the diameter $D_d = 2.5$ mkm, that is why such droplets were considered in computations. Comparison of the obtained results with experimental data of Trinks et al. presented in [14] is demonstrated in Fig. 2. Stratification of the two-phase flow is seen with limiting droplet trajectory corresponding to the angle 40° .

Simulation of Gas-Droplet Plume Flow

Calculations of the nozzle and plume flow of the gas-droplet mixture were performed for conditions of experimental setup of the Institute of Thermophysics (Novosibirsk, Russia). The nozzle flow parameters were as follows: the stagnation pressure was 3390 Pa, the total temperature was 293.15 K, the carrier gas was nitrogen, the nozzle-throat radius was 5 mm, the radius of the generatrix in the throat cross section was 5 mm, the radius of the exit cross-section was 9.55 mm, the Mach number at the nozzle exit was 2.84. Water droplets were considered, it

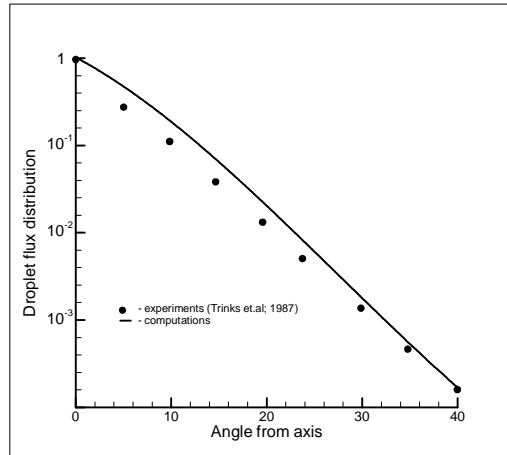


FIGURE 2. Angular distribution of the droplet flux in the plume flow [14].

was assumed that the droplets were originated in the critical cross-section of the nozzle, the droplet temperature and velocity were in equilibrium with those of the carrier gas.

For various initial droplet diameters figures 3 - 5 present pressure distributions and profiles of the probe droplet

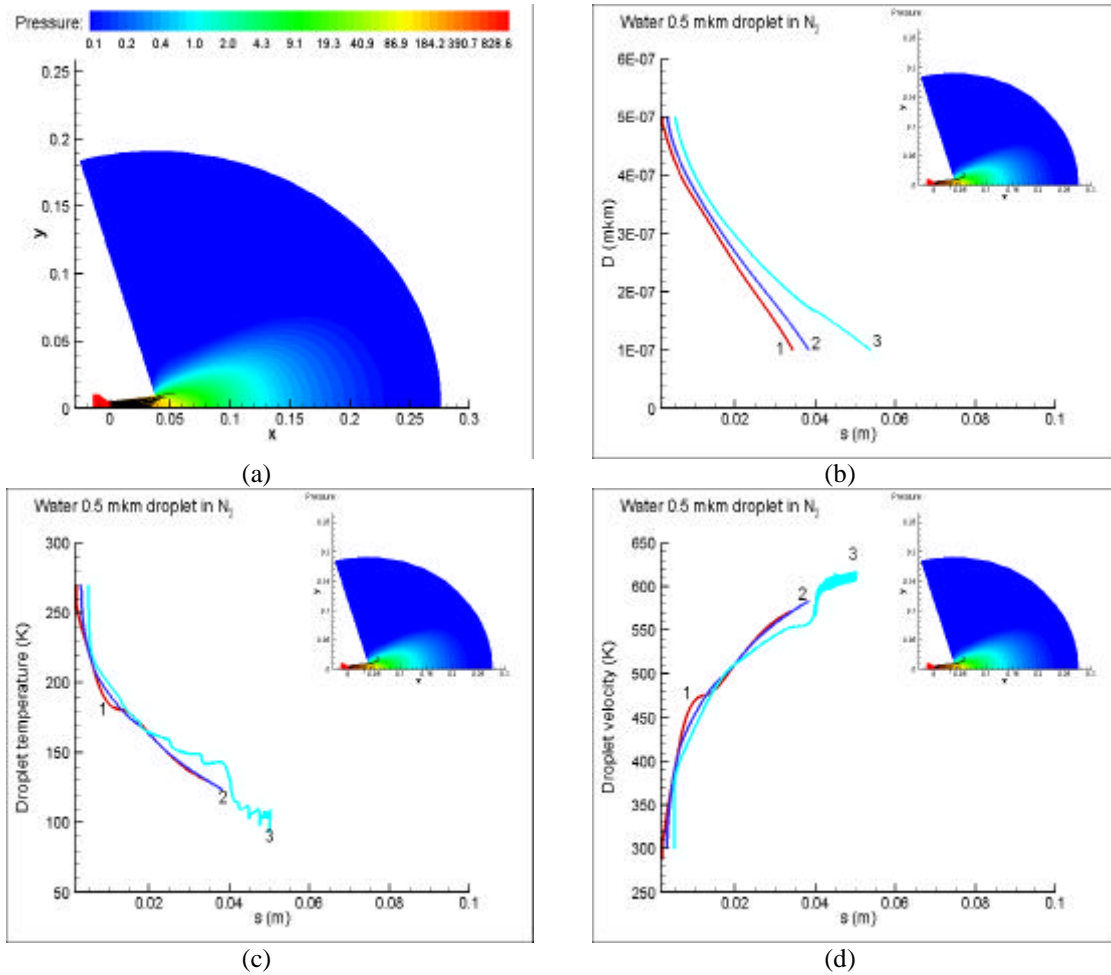


FIGURE 3. Nozzle and plume flow: pressure distribution and probe droplet trajectories, (a); variations of the droplet diameter, (b), the droplet temperature, (c), and the droplet velocity, (d), along characteristic trajectories. Carrier phase is nitrogen, water droplets, initial droplet diameter is 0.5 mkm.

diameter, temperature, and velocity along three characteristic trajectories (the profiles are depicted by red, blue, and light blue)

These cases correspond to various flow regimes characterized by complete droplet evaporation for $D_{d0}=0.5\text{mkm}$ and by practically absence of droplet evaporation for $D_{d0}=5\text{mkm}$.

Fig. 3 shows that the droplets in the core of the flow evaporate in the nozzle and for these droplets parameter distribution is closed to uniform. Only periphery droplets enter the plume flow. The flow is highly stratified in both axial and radial directions.

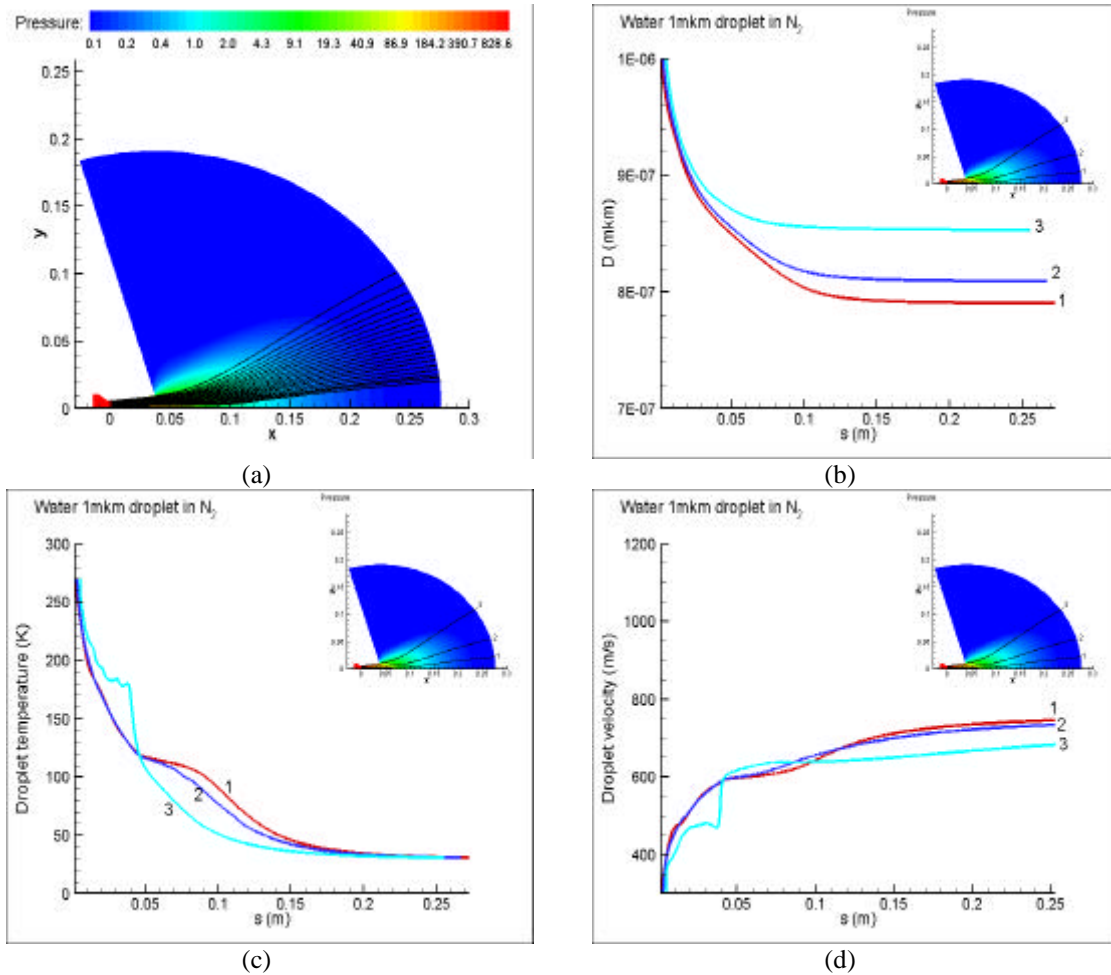


FIGURE 4. Nozzle and plume flow: pressure distribution and probe droplet trajectories, (a); variations of the droplet diameter, (b), the droplet temperature, (c), and the droplet velocity, (d), along characteristic trajectories. Carrier phase is nitrogen, water droplets, initial droplet diameter is 1 mkm.

Fig.4 presents flow parameters corresponding to droplets structure for droplet $D_{d0}=1\text{mkm}$. It is seen that in this case droplets in the core flow loss about 50% of their volume in the nozzle and in the vicinity of the nozzle exit. Downstream the flow the evaporation is negligible. Peripheral droplets undergo abrupt change of the temperature and velocity at the nozzle exit which is due to highly non-uniform structure of the carrier gas flow in this domain. The two-phase flow is stratified in radial direction.

Fig. 5 demonstrates that for parameters under study relatively large droplets, $D_{d0}=5\text{mkm}$, practically do not evaporate (loss of the volume is about 5%). Distribution of droplet parameters in this case is close to uniform. Comparing Figs. 4 and 5 it is worth to mention that in this case interphase relaxation of the temperature occurs faster than that of the velocity.

In all considered cases the flow about droplets is rarefied, in Fig. 6 Kn number distribution is presented for droplets with initial diameter 5 mkm.

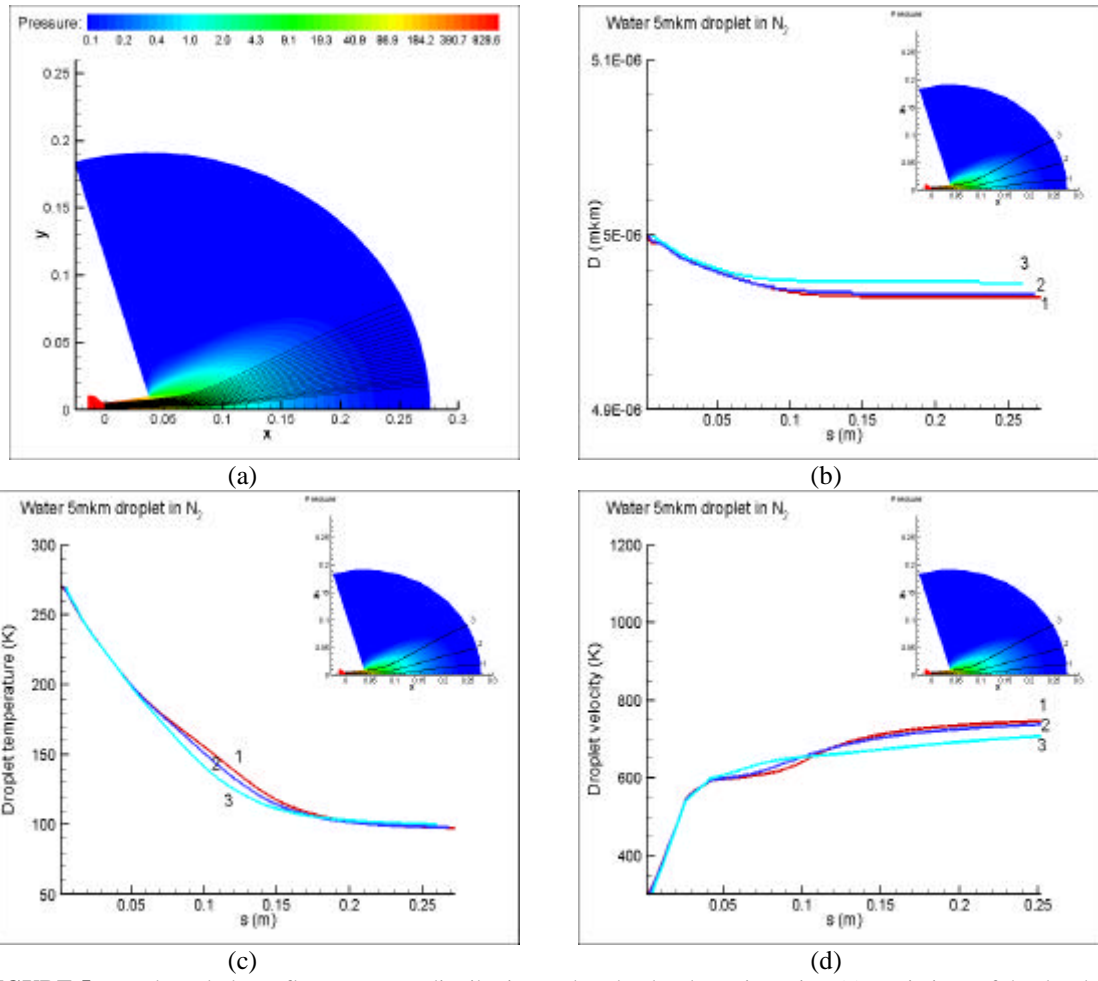


FIGURE 5. Nozzle and plume flow: pressure distribution and probe droplet trajectories, (a); variations of the droplet diameter, (b), the droplet temperature, (c), and the droplet velocity, (d), along characteristic trajectories. Carrier phase is nitrogen, water droplets, initial droplet diameter is 5 mkm.

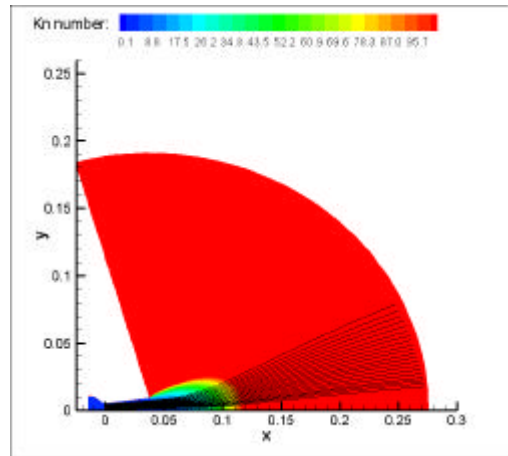


FIGURE 6. Kn number distribution for 5 mkm droplets in the nozzle and plume flow and probe droplet trajectories. Carrier phase is nitrogen, water droplets.

CONCLUSIONS

On the basis of analysis of phenomenological description of interphase mass momentum and heat transfer an Euler-Lagrange model was formulated to simulate nozzle and plume droplet flows in the transitional regime.

To validate the proposed model simulation of heating and evaporation of a droplet in a convective flow of ambient air as well as simulation of the angular distribution of the droplet mass flow rate in a two-phase plume flow were carried out. These simulations were performed in the framework of the one-way coupling approach, nevertheless, comparison of the obtained results with independent computations and available experimental data demonstrated good agreement for low and moderate evaporation rates.

Carrier and dispersed phase parameter distributions were obtained for three regimes of the two-phase flows in the nozzle and plume. Significant stratification of the flows was demonstrated.

Thus, the proposed model is able to provide adequate description of dilute two-phase nozzle and plume flows.

ACKNOWLEDGMENTS

This study is partially supported by the RFBR grants 05-01-00809 and 05-08-33420, as well as by the grant of the SPb Scientific Center of RAS. This support is gratefully appreciated.

REFERENCES

1. Yu.P. Golovachov, M.S. Ivanov, D.V. Khotyanovsky, A.N. Kudryavtsev, V.A. Mazurkevich, B.I. Reznikov, and A.A. Schmidt. "Numerical simulation of a multiphase three-component flow in a supersonic nozzle" *AIAA Paper 2003-3494*, 2003.
2. Yu.P. Golovachov, M.S. Ivanov, D.V. Khotyanovsky, A.N. Kudryavtsev, B.I. Reznikov, A.A. Smirnovsky, A.A. Schmidt. "Multiphase three-component nozzle flow (model validation)" *Proc. of European Congress on Computational Methods in Applied Sciences and Engineering ECCOMAS 2004*, edited by P. Neittaanmäki et al., (on CD), 2004
3. Nigmatulin R.I. *Dynamics of multiphase media*, Hemisphere, New York, Vol. 1 2, 1991.
4. Crowe C.T., Babcock W., Willoughby P.G. *Progr. Heat and Mass Transf.*, **8**, 419-429, (1973).
5. Hermesen R.W. "Review of particle drag models" in JANAF Performance Stand. Subcommittee 12th Meeting, pp. 113-134, 1979.
6. Gelfand B.E. *Progr. Energy Comb. Sci.*, **22**, 201-265, (1996)
7. Senkovenko S.A., Stasenko A.L. *Relaxation processes in supersonic gas jets*. M.: Energoatomizdat, 1985 (in Russian).
8. Renksizbulut M., Yuen M.C. *J. Heat Transfer*, **105**, 389-397, (1983)
9. Lu H.Y., Chiu H.H. *AIAA Journal*, **4**, 1008-1011, (1966)
10. Renksizbulut M., Yuen M.C. *J. Heat Transfer*, **105**, 384-388, (1983)
11. Cowe P.N., Claxton K.T., Lewis J.B. *Trans. Inst. Chem. Eng.*, **14**, (1965)
12. Cinar G., Yilbas B.S., Sunar M. *Int. J. Multiphase Flow*, **23**, 1171-1188, (1997)
13. Hadem J., Nikitin V.F. *Vestnik MGU, ser. 1. Matematika, mekhanika*, **40**, 33-40 (2005)
14. Genkin L., Baer V., Falcovitz F. *Shock waves*, **7**, 211-218, (1997)